Cloud Top Height Retrieval Using Polarizing Remote Sensing Data of POLDER

HE Xianqiang, BAI Yan, PAN Delu, ZHU Qiankun, and GONG Fang

State Key Laboratory of Satellite Ocean Environment Dynamics, Second Institute of Oceanography of State Oceanic Administration, Hangzhou 310012, China

Abstract   A retrieval method of cloud top heights using polarizing remote sensing is proposed in this paper. Using the vector radiative transfer model in a coupled atmosphere-ocean system, the factors influencing the upwelling linear polarizing radiance at top-of-atmosphere are analyzed, which show that the upwelling linear polarizing radiance varies remarkably with the cloud top height, but has negligible sensitivity with cloud albedo and aerosol scattering above the cloud layer. Based on this property, a cloud top height retrieval algorithm using polarizing remote sensing was developed. The algorithm has been applied to the polarizing remote sensing data of Polarization and Directionality of the Earth's Reflectances-2 (POLDER-2). The retrieved cloud top height from POLDER-2 compares well with the Moderate Resolution Imaging Spectroradiometer (MODIS) operational product with a bias of −0.83 km and standard deviation of 1.56 km.

Keywords: cloud top height, polarizing remote sensing, Polarization and Directionality of the Earth's Reflectances

Citation: He, X., Y. Bai, D. Pan, et al., 2009: Cloud top height retrieval using polarizing remote sensing data of POLDER, *Atmos. Oceanic Sci. Lett.*, **2**, 73–78.

1   Introduction

Clouds play an important role in the weather, climate change, and the earth's environment, because they strongly influence the incoming solar radiation and the outgoing thermal radiation (Weisz et al., 2007). Presently, cloud parameters on a global scale are derived by space-based observation. There are various techniques used to determine the cloud top height from space-based measurements, such as lidar (Winker and Trepte, 1998), stereo observations (Seiz et al., 2007), and a number of passive methods (Koelemeijer et al., 2002). For example, the CO_2-slicing technique was used to retrieve the cloud top height from Moderate Resolution Imaging Spectroradiometer (MODIS) data (Menzel et al., 1983; Wylie and Menzel, 1999), and the oxygen A band method was used for the Global Ozone Monitoring Experiment (GOME) satellite data (Burrows et al., 1999).

The Polarization and Directionality of the Earth's Reflectances (POLDER) instrument onboard the space-platform was serially launched by the French Space Agency; the instrument was designed to collect and

Corresponding author: HE Xianqiang, hexianqiang@sina.com.cn

measure the polarized and directional solar radiation reflected by the earth-atmosphere system (Deschamps et al., 1994). So far, three POLDER instruments have been launched. The POLDER-1 instrument was launched onboard the Advanced Earth Observing Satellite-I (ADEOS-I) in August 1996, which had collected the data almost continuously from October 1996 to June 1997; collection ended due to the failure of the solar panel in the platform. A similar instrument, POLDER-2, was launched in December 2002 onboard the ADEOS-II satellite. POLDER-2 continued the work of its predecessor until October 2003 when an electrical failure occurred. POLDER-3 was launched in December 2004 onboard the Polarization & Anisotropy of Reflectances for Atmospheric Sciences coupled with Observations from a Lidar (PARASOL) satellite; this unit is still operational today. For POLDER-1 and POLDER-2, the reflectance was measured at eight wavelengths: 443 nm (20 nm), 490 nm (20 nm), 565 nm (20 nm), 670 nm (20 nm), 763 nm (10 nm), 765 nm (40 nm), 865 nm (40 nm), and 910 nm (20 nm), where the first number is the wavelength of the center band, and the bracketed number is the bandwidth. Three bands (443 nm, 670 nm, and 865 nm) were used to measure the polarization of the reflected solar radiation. For POLDER-3, a band at 1020 nm was added, and the polarization bands were moved to 490 nm, 670 nm, and 865 nm. The POLDER data has been used to study several key scientific objectives related to climate change, and the cloud algorithms were presented by Buriez et al. (1997). In this paper, a retrieval method of cloud top heights by polarizing remote sensing was applied to the POLDER data and compared with the MODIS operational product.

2   Principle of cloud top height retrieval by polarizing remote sensing

In cloudy conditions, the upwelling linear polarizing radiance (LPR) at the top-of-atmosphere (TOA) is mainly contributed by the cloud reflection and the backscattering of the atmosphere molecule and aerosol above the cloud layer. Here, a vector radiative transfer numerical model in a coupled ocean-atmosphere system, called the Polarized Coupled Ocean-Atmospheric Radiative Transfer numerical model (PCOART) (He et al., 2007), is used to analyze the effects of cloud reflection, aerosol scattering, and cloud top height on the LPR at TOA. Hereafter, if there is no special mention, the wavelength considered is 443 nm,

and the incident solar irradiance at TOA is 1 mW cm^{-2} μm^{-1}.

2.1   Effect of cloud reflection on LPR

Because of the strong multi-scattering effect in the cloud layer, cloud top surface can be considered approximately as the Lambert surface, and its optical property can be directly described by the albedo. In order to test the effect of cloud reflection, we assumed a condition of 5 km cloud top height, 40° sun zenith angle, and a Rayleigh atmosphere with the optical thickness of 0.125. Figure 1 shows the variations of the upwelling total radiance (left column) and LPR (right column) at TOA with a sensor zenith angle under different cloud albedo (A) situations. It is easy to see that the upwelling total radiance is sensitive

to the cloud albedo, while the cloud albedo had a negligible effect on the LPR.

2.2   Effect of aerosol scattering on LPR

Generally, aerosol scattering usually affects the LPR at TOA when the cloud is low, because the great mass of aerosol often exists in the bottom of the atmosphere. For testing, we assumed a condition of 1 km cloud top height with the Rayleigh optical thickness of 0.2, and a troposphere background aerosol model with relative humidity of 80%. Figure 2 shows the variations of the LPR with sensor zenith angle at different aerosol optical thicknesses (AOT) above the cloud top, with the solar zenith angles of 30° and 60°. It can be seen that aerosol scattering also has a negligible effect on the LPR at TOA.
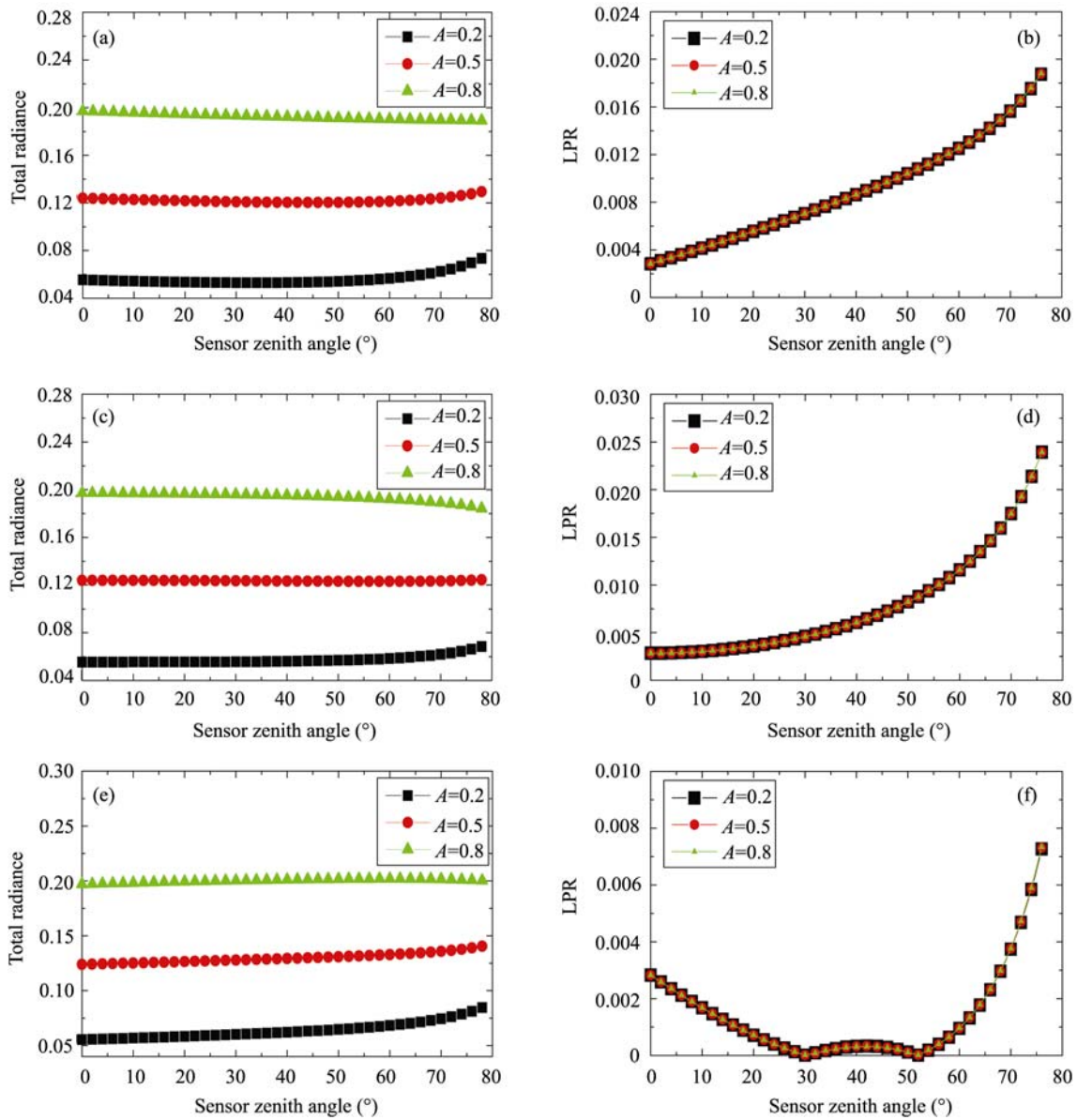

Figure 1   Variation of upwelling total radiances (Lt) and linear polarizing radiances (LPR) at TOA with different cloud albedos (A). (a) Lt with relative azimuth 0°, (b) LPR with relative azimuth 0°, (c) Lt with relative azimuth 90°, (d) LPR with relative azimuth 90°, (e) Lt with relative azimuth 180°, and (f) LPR with relative azimuth 180°.
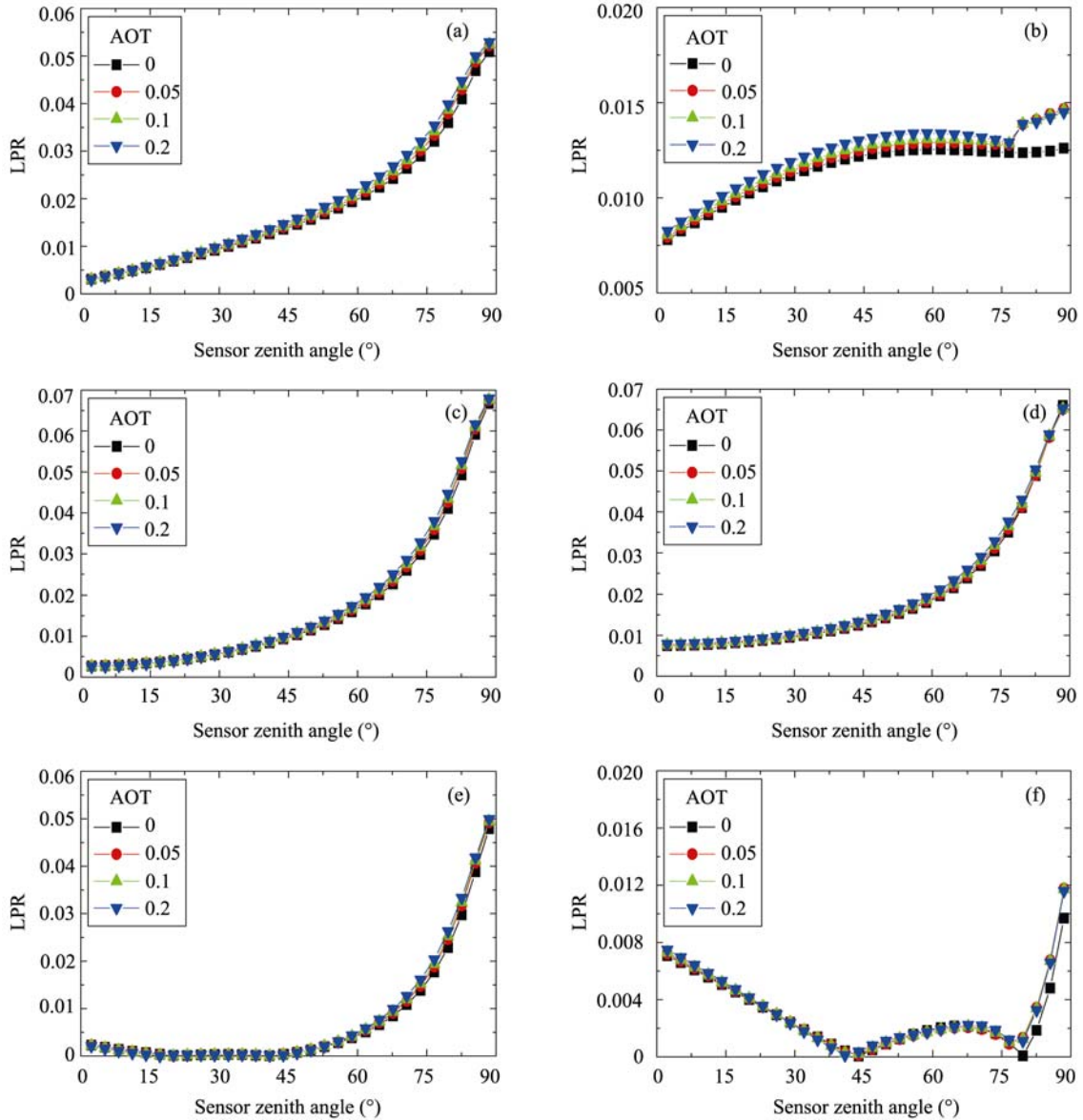
Figure 2 Variation of LPR with different aerosol optical thicknesses (AOT). (a) Sun zenith angle 30°, relative azimuth 0°; (b) sun zenith angle 60°, relative azimuth 0°; (c) sun zenith angle 30°, relative azimuth 90°; (d) sun zenith angle 60°, relative azimuth 90°; (e) sun zenith angle 30°, relative azimuth 180°; and (f) sun zenith angle 60°, relative azimuth 180°.

2.3   Effect of cloud top height or the Rayleigh scattering on LPR

For testing the effect of cloud top height, the LPR at TOA is calculated by PCOART with the cloud top height varying from 1 km to 15 km with a step of 2 km. From the sections 2.1 and 2.2, we knew that the LPR at TOA is not sensitive to the cloud albedo and the aerosol scattering, so we assume that cloud albedo is 0.8 with the Rayleigh atmosphere. Figure 3 shows the variations of the LPR with a sensor zenith angle at different cloud top heights with solar zenith angles of 10° and 70°. LPR varies remarkably with cloud top heights, and this property can be used to deduce the cloud top height. However, in some conditions (e.g., when the sensor zenith angle is less than 20°, as shown in Figs. 3a, 3c, and 3e), the

variation of LPR with cloud top height is very small limiting the inversion of cloud top height by the polarizing remote sensing method. However, this limitation can be solved by using the multi-angle viewing technique of the remote sensing sensor.

3   Algorithm of cloud top height retrieval by polarizing remote sensing

Using the above-mentioned analysis, we knew that LPR at TOA varied remarkably with the cloud top height at the ultraviolet or blue light wavelength with negligible sensitivity for the cloud albedo and aerosol scattering above the cloud layer. Therefore, the cloud top height can be retrieved by the Rayleigh scattering optical thickness above the cloud layer. The detailed processes for the
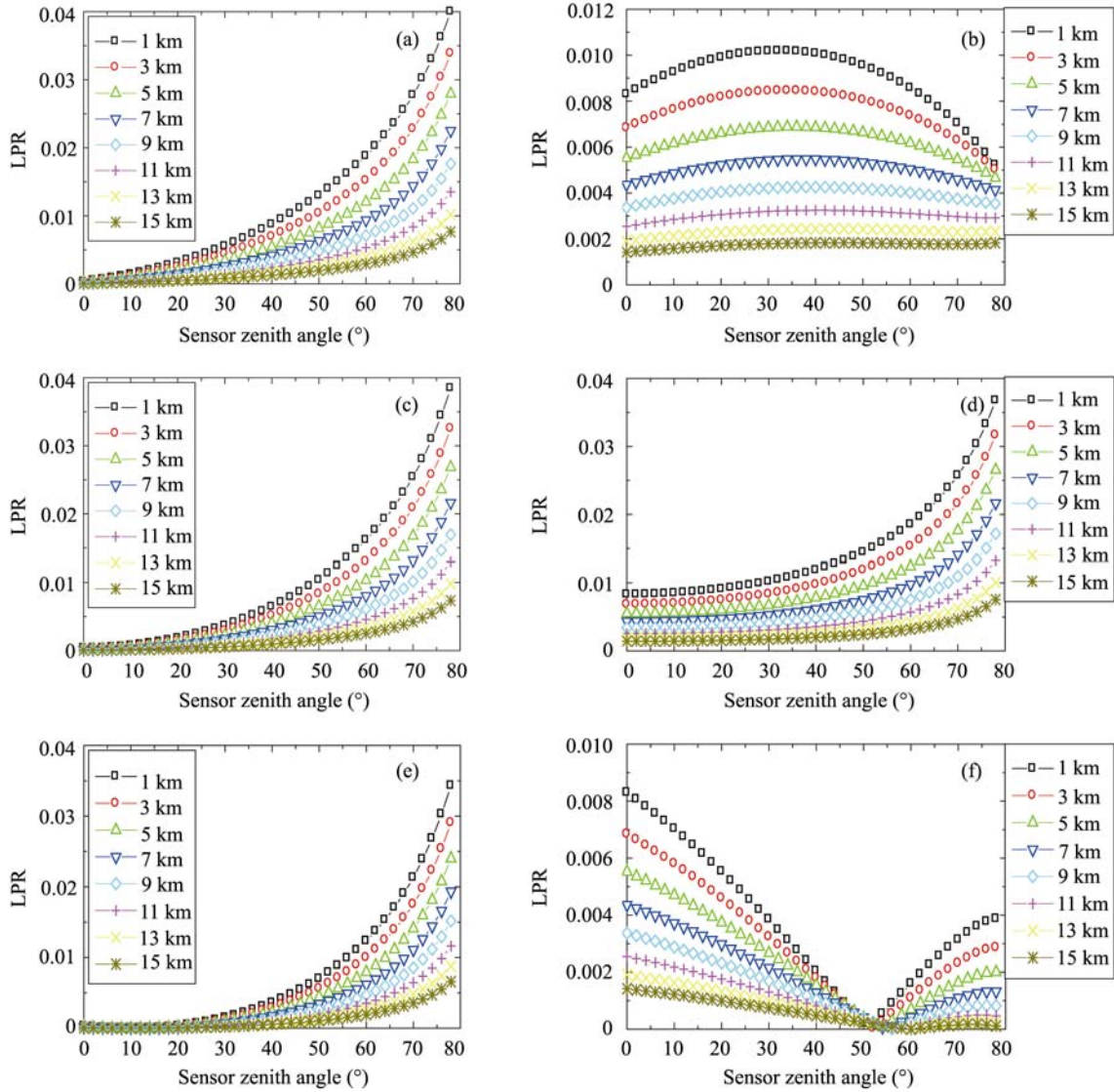
Figure 3 Variation of LPR with cloud top height. (a) Sun zenith angle 10°, relative azimuth 0°; (b) sun zenith angle 70°, relative azimuth 0°; (c) sun zenith angle 10°, relative azimuth 90°; (d) sun zenith angle 70°, relative azimuth 90°; (e) sun zenith angle 10°, relative azimuth 180°; and (f) sun zenith angle 70°, relative azimuth 180°.

cloud top height retrieval by the polarizing remote sensing are as follows:

(1) According to the band-setting of the satellite polarizing sensor, the ultraviolet or blue light wavelength band is chosen for the retrieval of cloud top height.

(2) The vertical profile of Rayleigh scattering optical thickness at the chosen band is determined. It can use the average values of the six atmosphere models, namely: the United Sates Standard Atmosphere Model (US62), Tropic Atmosphere Model (TROPIC), Middle latitude Summer Atmosphere Model (MIDSUM), Middle latitude Winter Atmosphere Model (MIDWIN), Sub-Arctic Summer Atmosphere Model (SUBSUM), and Sub-Arctic Winter Atmosphere Model (SUBWIN). The relative errors using the average values are less than 10%, and less than 5% when the cloud top height is less than 5 km.

(3) The vector radiative transfer equations of atmosphere are solved numerically with the bottom boundary of cloud surface to generate the look-up table of LPR at TOA with various geometrical situations between sun, sensor, and the cloud top heights.

(4) According to the geometries between sun and sensor at each cloudy pixel, the LPR at different cloud top heights is calculated by the look-up table. The best height as the final cloud top height value is chosen, with which the corresponding LPR in the look-up table is closest to the satellite-received LPR.

4 Application of the Algorithm to POLDER and validation

We used the polarizing remote sensing data of POLDER-2 onboard the ADEOS-II satellite to generate the cloud top height image with our algorithm. POLDER-2 has the capability of multi-angle viewing with up to 14 different viewing directions. According to

the analysis in section 2.3, the viewing angle at which LPR has the most significant variation with the cloud top height should be chosen. With the linear polarizing radiance data at the 443 nm band and the cloud pixel recognition, we chose the best geometric angle from the multi-angle viewing directions and then obtained the most approximate cloud top height value from the look-up table according to the linear polarizing radiance. Figure 4a displays the global cloud top height retrieved by the POLDER-2 data on 10 July 2003. It can be seen that the proposed method in this paper can effectively retrieve the cloud top height.

For the algorithm validation, the derived cloud top heights by the POLDER-2 data were compared with the Terra/MODIS operational cloud-top pressure product with collection 5. Because of the same equatorial crossing time at 1030 LST with the descending node, the change of clouds between POLDER-2 and Terra/MODIS images can be neglected. MODIS cloud top pressure was determined by the CO_2-slicing technique, which used radiances measured at the spectral bands located within the 15-μm broad CO_2 absorption region (Menzel et al., 2008). MODIS operational cloud top pressure product was derived globally with the spatial resolution of 5 km (level-2 products) and binned to a 1° equal-angle grid (level-3 product), which were available for daily, 8-day, and monthly time periods. Generally, the MODIS cloud top pressure products were converted to the cloud top heights by the National Center for Environmental Prediction (NCEP) Global Forecast System, which provided the girded temperature profiles every 6 hours. In order to obtain more comparable results, we used the same pressure profile as the proposed algorithm in this paper (i.e.,
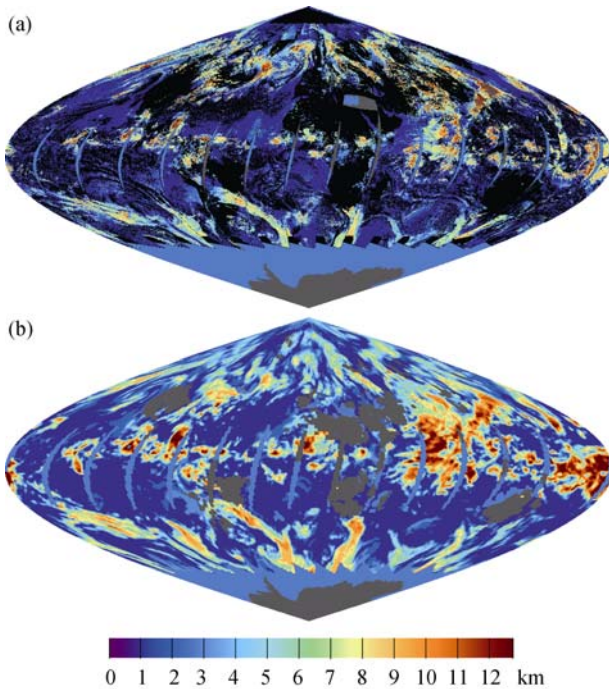
the average pressure profile of the six atmosphere models). Also, in order to compare the two values on a pixel-by-pixel basis, the MODIS cloud top height data was re-projected onto the POLDER latitude-longitude grid using the weighted average method. Figure 4b displays the Terra/MODIS cloud top height image on 10 July 2003, and Figure 5 shows the scatter-plot of cloud top height retrieved by POLDER-2 and Terra/MODIS on 10 July 2003. We could see that the cloud top heights derived from POLDER-2 using the proposed method in this paper are consistent with the MODIS operational product with a bias of −0.83 km and the standard deviation of 1.56 km for ~4023 pixels. The dispersions are partly due to the retrieval algorithm differences and partly due to the inaccuracy cloud mask.

5 Conclusion

Cloud top height information is critical for numerical weather forecasting, climate modeling, atmospheric research, and is also helpful for navigational alarms and thunderstorm prediction. In this paper, a retrieval method of cloud top heights was proposed using polarizing remote sensing. Using the vector radiative transfer numerical model in a coupled atmosphere-ocean system (PCOART), the factors affecting the upwelling linear polarizing radiance at top-of-atmosphere are analyzed, and show that the upwelling linear polarizing radiance at TOA varies remarkably with the cloud top height, but has negligible sensitivity to the cloud albedo and the aerosol scattering above the cloud layer. Based on this property, a cloud top height retrieval algorithm was developed by the polarizing remote sensing. First, the look-up table of LPR at TOA with various geometries of sun and sensor and the cloud top heights was generated by solving the vector radiative transfer equations of atmosphere with the bottom boundary of cloud surface. Then, according to the geometry between sun and sensor at each cloudy pixel, the LPR at different cloud top heights was calculated with the look-up table, and the best value was chosen as the final cloud top height value, with which the corresponding LPR in look-up table was closest to the satellite-received LPR. The algorithm was applied to the polarizing
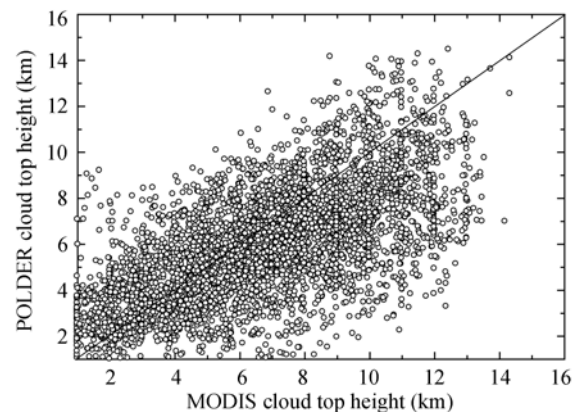

Figure 4 Global cloud top height retrieval by (a) POLDER-2 and (b) Terra/MODIS on 10 July 2003.

Figure 5 Scatter-plot of cloud top height retrieved from POLDER-2 and Terra/MODIS on 10 July 2003.

remote sensing data of POLDER-2. By comparing with the MODIS operational cloud-top height product, the cloud-top heights derived from POLDER-2 using the proposed method in this paper were very good and had a bias of −0.83 km and standard deviation of 1.56 km. The dispersion originated in part from the differences between the retrieval algorithm and in part from the inaccuracy cloud mask.

References

Buriez, J. C., C. Vanbauce, F. Parol, et al., 1997: Cloud detection and derivation of cloud properties from POLDER, *Int. J. Remote Sens.*, **18**, 2785−2813.

Burrows, J. P., M. Weber, M. Buchwitz, et al., 1999: The Global Ozone Monitoring Experiment (GOME): Mission concept and the first scientific results, *J. Atmos. Sci.*, **56**, 151−175.

Deschamps, P. Y., F. M. Breon, M. Leroy, et al., 1994: The POLDER mission: Instrument characteristics and scientific objectives, *IEEE Trans. Geosci. Remote Sens.*, **32**, 598−615.

He, X., D. Pan, Y. Bai, et al., 2007: Vector radiative transfer numerical model of coupled ocean-atmosphere system using matrix-operator method, *Science in China Series D: Earth Sciences*, **50**(3), 442−452.

Koelemeijer, R. B. A., P. Stammes, J. W. Hovenier, et al., 2002: Global distributions of effective cloud fraction and cloud top pressure derived from oxygen A band spectra measured by the Global Ozone Monitoring Experiment: Comparison to ISCCP data, *J. Geophys. Res.*, **107**, D124151, doi:10.1029/2001JD000840.

Menzel, W. P., R. A. Frey, H. Zhang, et al., 2008: MODIS global cloud-top pressure and amount estimation: Algorithm description and results, *J. Appl. Meteor. Climatol.*, **47**, 1175−1198.

Menzel, W. P., W. L. Smith, and T. R. Stewart, 1983: Improved cloud motion wind vector and altitude assignment using VAS, *J. Appl. Meteor.*, **22**, 377−384.

Seiz, G., S. Tjemkes, and P. Watts, 2007: Multiview cloud-top height and wind retrieval with photogrammetric methods: Application to Meteosat-8 HRV observations, *J. Appl. Meteor. Climatol.*, **46**, 1182−1195.

Weisz, E., J. Li, W. P. Menzel, et al., 2007: Comparison of AIRS, MODIS, CloudSat and CALIPSO cloud top height retrievals, *Geophys. Res. Lett.*, **34**, L17811, doi:10.1029/2007GL030676.

Winker, D. M., and C. R. Trepte, 1998: Laminar cirrus observed near the tropical tropopause by LITE, *Geophys. Res. Lett.*, **25**, 3351−3354.

Wylie, D. P., and W. P. Menzel, 1999: Eight years of high cloud statistics using HIRS, *J. Climate*, **12**, 170−184.